Investigation on the swelling behaviour in poly(dimethylsiloxane) rubber networks using nmr and compression measurements

Heike Menge[a],[*], Sabine Hotopf[a], Steffen Pönitzsch[b], Sven Richter[b], Karl-Friedrich Arndt[b], Horst Schneider[a], Uwe Heuert[a]

[a]*Martin-Luther-Universität Halle-Wittenberg, Fachbereich Physik, Friedemann-Bach-Platz 6, D-06108 Halle/Saale, Germany*
[b]*Technische Universität Dresden, Institut fhr Physikalische Chemie und Elektrochemie, Mommsenstraße 13, D-01069 Dresden, Germany*

Abstract

Recent investigations on elastic behaviour, using uniaxial compression measurements of the swelling degree of poly(dimethylsiloxane) rubber (PDMS) networks lead to the assumption that a transition from the affine to the free-fluctuating phantom network occurs. To study the swelling process in different solvents, PDMS networks with different crosslink densities, molecular weight distributions and memory terms were synthesized. Additionally, another fast method for network characterization is given by the analysis of the transversal nmr relaxation. For elastomer networks, well above the glass transition temperature T_g, the presence of topological constraints and permanent crosslinks leads to a non-zero average of homo- and hetero-nuclear interactions, which results in a solid-like relaxation behaviour. The shape of the decay of proton transversal magnetization, using the Hahn echo sequence in the dry PDMS network, is related to the crosslink density. The results of the nmr experiments are compared with compression measurements on dry and swollen networks. © 1999 Elsevier Science Ltd. All rights reserved.

Keywords: PDMS networks; Nmr; Swelling

1. Introduction

Different methods have been developed to obtain exact network parameters and to get a better understanding of the correlation between structure and properties. The measurement of the variation of swelling degree with the elastic behaviour is, among others, one of the most powerful and efficient methods for determining the crosslink densities or molecular masses of network chains. Early measurements on dry and swollen networks indicated a change in the rubber elasticity with swelling [1,2], though it should be noted that the swelling behaviour depends on the chemical nature of the networks and the solvent [3]. From the theory of rubber elasticity a relationship between the crosslinking density and the shear modulus of a network can be obtained. The modulus can easily be measured by uniaxial compression. In order to calculate the M_c value assumptions on the deformation behaviour of the network are imperative.

In an earlier paper [4] it was shown that the elastic behaviour is a function of the swelling degree, i.e. it depends on the swelling agent. The molecular weight M_c between two crosslinks calculated from the elastic behaviour (phantom model) as a function of the swelling degree was described by two regimes. The strong increase of the calculated M_c in the range of small swelling degrees was explained by a transition from an affine to a free-fluctuating network. The slow rise at larger swelling degrees seems to result from a change in the memory term. These explanations have to be proved by further experiments. Therefore, to study the swelling process in different solvents, poly(dimethylsiloxane) rubber (PDMS) networks with different crosslink densities, molecular weight distributions and memory terms were synthesized. Additionally, we were looking for another method to estimate the crosslink densities of rubber networks. Several papers [5–11] have shown that the measurement of transversal [1]H-nmr relaxation is a successful method of investigating the structural and motional parameters in polymer networks at temperatures well above the glass transition temperature T_g [6,8]. The presence of topological hindrances leads to an anisotropic segmental motion, which results in a non-zero average of dipolar coupling. Using this residual dipolar magnetic interaction of protons, a number of papers [5–9,12,13] describe and test several

* Corresponding author. Tel.: + 49-345-5525595; fax: + 49-345-5527161.

approaches to the determination of the molecular mass between two crosslinks M_c in different elastomeric polymer networks like natural rubber (NR), butadiene rubber (BR), styrene–butadiene rubber (SBR) and PDMS.

The aim of this work is to compare the molecular masses of the network chains determined with the nmr and compression methods. Furthermore, the influence of the network structure on the results was investigated. In the literature [5–7,14,15] a good agreement between the results of conventional methods (stress–strain measurements, swelling, G-modulus) with nmr results has been obtained.

2. Theory

Anisotropic nuclear interactions, such as dipole–dipole or quadrupolar couplings, are a source of information concerning not only the structure and bonding but also the rate and the nature of molecular motions [13,16–18]. The transversal [1]H-nmr relaxation is mainly determined by the dipolar magnetic interaction of protons. Therefore, for elastomers well above T_g a motional averaging of this interaction, and consequently the nuclear motion itself, is detectable in this way.

The starting point is the secular part of the dipolar (or quadrupolar) Hamiltonian

$$\omega(\vartheta) = \Delta P_2(\cos \vartheta) \quad (1)$$

where $\Delta = \mu_0 \gamma^2 \hbar / (4\pi r^3)$ and ϑ is the angle between the static magnetic field B_0 and the vector of dipolar coupling along the nuclear connecting vector $\boldsymbol{a}$ ($|\boldsymbol{a}| = r$).

For an isotropic rigid lattice of spin pairs we get [19,20] $[P_2(\cos \vartheta)]^2 = 1/5$ and

$$M_2 = \frac{9}{4} \langle [\omega_R(\vartheta)]^2 \rangle = \frac{9}{20} \Delta^2 \quad (2)$$

for the second moment. In the case of a very fast ($\nu_{ai} > 10^6 \text{ s}^{-1}$) anisotropic motion (like in network chains consisting of N_S freely jointed segments of length b with an end-to-end vector R ($R^2 = N_S b^2$)) the dipolar interaction is reduced [12,20] and this results in a 'residual non-averaged by this fast anisotropic reorientation part of the second moment' [21,22] M_2^{Res}

$$M_2^{Res} = \frac{9}{4} \langle [\omega_R(\vartheta)]^2 \rangle = \frac{9}{20} \Delta^2 \left(\frac{3}{5N_S} \right)^2 \quad (3)$$

In elastomers well above T_g it is usual to define an anisotropy parameter $q = M_2^{Res}/M_2$ which reflects the residual dipolar or quadrupolar spin interaction relatively to the second moment in a rigid lattice. This is caused by fast anisotropic segmental motions due to topological constraints, such as chemical crosslinks or entanglements, and results in a solid-like relaxation behaviour. This anisotropy parameter q is sensitive to the crosslink density [20].

The interpretation of transversal nmr relaxation, which has been used in the following work, is based on a modified single chain model where the protons of the hydrocarbons are taken as probes for the nmr measurement. This model was successfully tested earlier [5–7,9] and has been described in full detail in Refs. [10] and [11]. Here only the main features are summarized. The theory is based on the following assumptions.

1. The network consists of intercrosslink chains and dangling ends with different restrictions of the molecular mobilities. Consequently, the corresponding transverse relaxation signals are different in shape and time behaviour.
2. Real chains are replaced by non-interacting Kuhn chains [23] consisting of N_S freely jointed statistical segments with protons which interact along the segment axis.
3. Intercrosslink chains are fixed at both ends. The motional statistics provide a mean, small anisotropy of the fast local motion (correlation time τ_{fast} in the order of 10^{-9} s) of the Kuhn statistical segments [23]. Thus, a small part of the dipolar interaction is left and expressed as the ratio q of the remaining second moment M_2^{Res} and the second moment M_2 of the rigid lattice.
4. The remaining dipolar interaction can only be diminished by an overall isotropic motion of the whole intercrosslink chain. As a result of the larger size of the moving object the correlation time τ_{slow} of this motion is in the order of 10^{-3} s.
5. Dangling ends are fixed only at one side. Their segmental motion is nearly isotropic ($q \approx 0$). Consequently, the dipolar interaction is already averaged to zero by this process.

For rubber networks, the range of molecular dynamics is intermediate between the motional narrowing and the rigid lattice case. The transversal relaxation $M(t)$ for correlation times τ_c much greater than the Larmor period ($\omega_0 \tau_c \gg 1$) is well described by the Anderson–Weiss formula [19]:

$$M(t) = M(0) \exp \left[\int_0^t G(\tau)(t - \tau) \, \mathrm{d}\tau \right] \quad (4)$$

Assuming a simple exponential correlation function $G(\tau) = M_2 \exp(-\tau/\tau_c)$, the transverse relaxation function is given by

$$M(t) = \exp \left\{ -M_2 \tau_c^2 \left[\exp \left(-\frac{t}{\tau_c} \right) + \frac{t}{\tau_c} - 1 \right] \right\} \quad (5)$$

If the correlation time is much shorter than the observation time ($\tau_c \ll t$ (decay time); ω_0 is the Larmor frequency), the Bloembergen–Purcell–Pound (BPP) formula [19] is valid (again assuming a simple exponential correlation function):

$$\frac{1}{T_2(\tau_c)} = \frac{1}{3} M_2 \tau_c \left[3 + \frac{5}{1 + (\omega_0 \tau_c)^2} + \frac{2}{1 + (2\omega_0 \tau_c)^2} \right] \quad (6)$$

and a single-exponential decay appears: $M(t) \sim \exp(-t/T_2)$. The intermediate case, if both conditions are fulfilled, follows by use of Eqs. (5) and (6): $M(t) \sim \exp(-tM_2\tau_c)$.

Table 1
Characterization of the molar mass of the starting materials by SEC, VPO, SLS[a]

Polymer	M_w(SEC) (10^3 g mol^{-1})	M_n(SEC) (10^3 g mol^{-1})	Dispersity	M_n(VPO) (10^3 g mol^{-1})	M_w(SLS) (10^3 g mol^{-1})
1	7.1	3.2	2.237	2.3	—
2	70	19	3.661	10.3	58.5
3	137	27	5.114	8.0	100
4	221	18	11.977	8.2	207

[a] SEC: size exclusion chromatography; VPO: vapour pressure osmometry; SLS: static light scattering.

Taking into account assumptions (1)–(5) above, appropriate correlation functions can be derived [10,24] that relate the molecular dynamics with nmr relaxation parameters. For intercrosslink chains this correlation function is given by

$$G(\tau) = M_2\left[(1-q)\exp\left(-\frac{\tau}{\tau_{fast}}\right) + q\right]\exp\left(-\frac{\tau}{\tau_{slow}}\right) \quad (7)$$

and can be approximated for $q \ll 1$ and $\tau_{fast} \ll \tau_{slow}$ by

$$G(\tau) \propto M_2\exp\left(-\frac{\tau}{\tau_{fast}}\right) + qM_2\exp\left(-\frac{\tau}{\tau_{slow}}\right) \quad (8)$$

This leads to a Gaussian-like relaxation function. For the dangling ends, there is no reason for an anisotropy of local motion ($q \approx 0$). Therefore, their magnetization decay is purely exponential (liquid-like).

Usually a second, very long exponential tail (liquid-like; relaxation time $T_{2,sol}$) of an amount smaller then 5% can be detected. This tail (fraction C) could be eliminated or reduced by an extraction procedure and, consequently, belongs to sol molecules or admixtures of high mobility.

Then the total transversal magnetization decay is composed of all three contributions

$$M(t) = A\,M(t)_{NW} + B\,M(t)_{DE} + C\,M(t)_{Sol}$$

and is given by [10,24]

$$M(t) = A\exp\left\{-\frac{t}{T_2(\tau_{fast})}\right.$$
$$\left. - qM_2\tau_{slow}^2\left[\exp\left(-\frac{t}{\tau_{slow}}\right) + \frac{t}{\tau_{slow}} - 1\right]\right\}$$
$$+ B\exp\left[-\frac{t}{T_2(\tau_{fast})}\right] + C\exp\left(-\frac{t}{T_{2,sol}}\right) \quad (9)$$

The fractions A, B and C represent the parts of magnetization of protons in intercrosslink chains, dangling ends and 'sol'-fraction (free chains) corresponding in first approximation to the molecular mass parts. The problems of determination of the second moment of the rigid lattice are given in detail in an earlier paper [10].

For the first moment, Eq. (9) seems to be too complicated and contains too many parameters for a fit of the transversal relaxation curve. However, the signal was measured in a large time window: the initial delay is about 40 μs, the longest delay 100–200 ms. That means, many groups, measuring up to about 3 ms, consider the A-term only and neglect the signal parts of the dangling ends (B) and the free chains (C). These exponential tails can be separated relatively easily. Secondly, the nature of the slower process, which averages the interaction to zero, is often unknown. But, for the determination of the remaining part of the second moment after the faster, anisotropic molecular reorientation, this does not play any role. Additionally, a signal-to-noise of 1000 to 10 000 is necessary to analyse the relaxation curves by using a model with a large number of parameters. Therefore, often it is quite sufficient to assume that the slower correlation time is larger then the measuring time. Thus, mainly, two parameters, the short correlation time τ_{fast} and the anisotropy q, were measured.

Based on the idea by Gotlib et al. [24], that the factor q is the ratio between the second moments well above the glass transition temperature and those of the rigid lattice, the averaged molecular mass of intercrosslink chains M_c can be determined. It is assumed that the polymer chain consists of N_S Kuhn statistical segments. It follows [9–11,20] that

$$M_c = \frac{k}{\sqrt{q} - \sqrt{q_0}}\,\frac{3}{5}\,c_\infty\,\frac{M_{ru}}{N} \quad (10)$$

where M_{ru}/N is the molecular mass of one monomer unit per number of backbone bonds in one unit. The quantity c_∞ is the number of backbone bonds in one Kuhn segment. The contribution of entanglements is described by the value $q = q_0$ evaluated by fitting the relaxation decay of the uncrosslinked sample using Eq. (9). This q_0-correction is only necessary if the weight of molecular mass of the prechains is more than that of the entanglements.

The prefactor k depends on the direction between the spin–spin connecting vector and the segment direction. If the H–H-connecting vector is parallel to the segment axis, then $k = 1$ (in the perpendicular case the prefactor is only $1/2$). In the case of the PDMS under study, the prefactor k is averaged to $1/4$ with the assumption that the segment direction lies in the HHH-plane spanned by the protons of the methyl groups.

In the limit $\tau_{slow} \gg t$, the contribution of just the intercrosslink chains to Eq. (9) is equal to the expression [12,25] given by Sotta and Fülber for the short time behaviour of

Table 2
Sample characterization by nmr and compression measurements at different swelling degrees. THF: tetrahydrofuran; r.t.: room temperature

Sample	Polymer	η ($h^{2/3}$)	$\phi_{polymer}$	M_c(dry) (nmr,60°C) (g mol^{-1})	M_c(app., dry) (compress., r.t.) (g/mol)	Swelling degree in			M_c(app.) at r.t. (g mol^{-1})			
						acetone	toluene	THF	acetone (compress.)	toluene (compress.)	THF (compress.)	acetone (nmr)
36	4	1	1	12 100	15 000	1.35	7.4	8.5	20 000	40 000	—	12 600
5	2	1	1	8200	6000	1.39	4.76	5.51	8900	15 200	19 000	7800
48	2	0.8	0.715	9950	6700[c]	1.55	5.57	6.88	13 200	22 650	20 000	—
46	2	0.6	0.464	13 100	6100[c]	1.48	6.85	8.76	13 100	24 100	22 500	—
44	2	0.4	0.253	13 800	5500[c]	1.5	7.36	9.01	8600	14 200	17 100	—
38	2 (53 wt%) 4 (47 wt%)	1	1	8100	10 850	1.345	4.25	5.05	11 000	11 900	9500	7500
40	2 (27 wt%) 4 (73 wt%)	1	1	10 700	10 150	1.30	4.7	5.22	10 600	15 200	10 750	9200
42	2 (9 wt%) 4 (91 wt%)	1	1	12 100	12 300	1.42	5.14	6.03	13 000	24 300	22 100	—
50	1 (66 wt%) 2 (34 wt%)	1	1	2010[a]	2600[b]	1.38	2.50	2.63	2900[b]	1800[b]	2400[b]	1730[a]
51	1 (66 wt%) 3 (34 wt%)	1	1	1920[a]	2200[b]	1.35	2.58	2.94	2100[b]	2500[b]	2400[b]	2030[a]
52	1 (66 wt%) 4 (34 wt%)	1	1	1920[a]	2550[b]	1.38	2.69	3.03	2000[b]	4400[b]	2800[b]	1990[a]

[a] At the limit $\tau_{slow} \ll t$ Eq. (9) yields: $M(t) = A[\exp(-t/T_2) - qM_2 t^2/2] + B\exp(-t/T_2) + C\exp(-t/T_2^{sol})$.

[b] From Ref. [4] for the sample nos 50, 51 and 52 the value $A = 0.5$ is predicted.

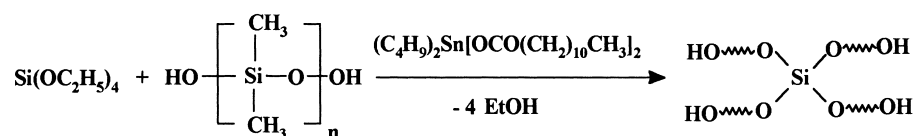[c] The M_c values are corrected by η (see Eqs. (11a) and (11b)).

their model introducing a Gaussian distribution of the end-to-end vector.

3. Experimental

3.1. Samples:

The PDMS networks were obtained by crosslinking various α,ω-dihydroxypolydimethylsiloxanes (Table 1) with different precursor chain lengths in the presence of the tetra-functional crosslinking agent tetraethoxysilane. The crosslinking agent was added in equimolar quantities. The catalyst for this synthesis was 1 wt% dibutyltin didodecanoate.

Firstly, the α,ω-dihydroxypolydimethylsiloxanes were investigated in toluene:

using the Hahn echo sequence. Samples were swollen in different deuterated solvents until the equilibrium swelling degree was reached (acetone, toluene, THF) and the swelling ratio was determined.

Compression measurements were carried out on both dry and swollen samples at 293 K.

The swelling degree was determined gravimetrically and also optically with a cathetometer. The applied forces were in the range of 20 to 300 N ($1 < \lambda^{-2} < 1.2$). In all cases a linear relationship was found, the requirement for the evaluation of the data with Eqs. (11a) and (11b).

The relationship between stress and uniaxial deformation with respect to measurements of swollen networks is given by Eqs. (11a) and (11b). All quantities (area, crosslink density) refer to the dry state (for details see Refs. [4,26]).

The measurements were carried out using a modified FICA 50 light scattering apparatus (SLS-Systemtechnik, Freiburg, Germany), a Knauer vapour pressure osmometer and a Waters Size Exclusion Chromatograph.

The chromatograms of the polymers 1–4 show a distinct portion of cycles in the polydimethylsiloxanes. The M_n (SEC) are calculated without this portion. This is the reason for the difference between M_n(VPO) and M_n(SEC). These cycles are not able to react with the crosslinking agent. The polymers 2 and 4 were crosslinked separately without any solvent and the sample nos 5 and 36 were obtained. Secondly, the polymer 2 was crosslinked in the presence of cyclohexane with different polymer concentrations ϕ_{polymer} (sample nos 44, 46 and 48). Thirdly, two series of bimodal samples were synthesized. In the first series (sample nos 38, 40 and 42) networks were built by mixing a certain ratio of polymers 2 and 4 to achieve different distributions and average values of molar masses. In a second series (sample nos 50, 51 and 52) two parts of the polymer 1 and one part of a second polymer, either 2, 3 or 4, were combined.

The samples were sliced into small cylinders (with a height and diameter of approximately 2 mm and 5 mm respectively). In order to remove unreacted siloxanes, the samples were extracted for several days with toluene and then deswollen with a toluene–methanol mixture, steadily increasing the fraction of methanol.

The nmr measurements were performed on a Varian Unity 400 spectrometer operating at a 400 MHz proton frequency. All relaxation curves were taken at 300 K. Transversal magnetic relaxation decays were obtained by

$$\sigma = \frac{f}{A_0} = (A\eta\nu_P RTQ^{1/3})|\lambda - \lambda^{-2}| \tag{11a}$$

$$G* = G_0 Q^{-1/3} = \frac{f/A_0}{Q^{1/3}|\lambda - \lambda^{-2}|} = A_f \eta\nu_P RT$$

$$= A_f \eta\rho_P RT/M_c \tag{11b}$$

σ is the stress, f is the force, A_0 is the area, A_f is a microstructure factor, η is a memory term (often $h^{2/3}$), ν_P is the crosslink density (ρ_P/M_c), R is the gas constant, T is the absolute temperature, M_c is the molecular weight between crosslinks, ρ_P is the density of the network ($0.976 \pm 0.015 \text{ g cm}^{-3}$), λ is the deformation, Q is the equilibrium swelling degree and G_0 is the modulus per unit area of unstrained dry gel.

4. Results

The analysis of the compression measurements requires some assumptions on the deformation behaviour. Only if η is known, and assumptions about the microstructure factor are made, is it possible to calculate molecular weights of network chains. Two limit cases exist in the picture of the phantom network: the affine (e.g. Herrmans–Flory–Wall, $A_f = 1$) and the free-fluctuating limit (e.g. James–Guth, A_f depends on the functionality f of the network, $A_f = (1–2/f)$ [26,27]. The M_c (compression) values in Table 2 were calculated according to Eqs. (11a) and (11b) using the experimentally estimated modulus $G*$ and under the assumption that $A_f = 1$. Therefore, they are only apparent values. It

Table 3
Network analysis of the nmr transversal relaxation in the dry state using Eq. (9)

Sample	C^{Sol} (%)	T_2^{Sol} (ms)	B (%)	T_2 (ms)	τ_{slow} (ms)	A (%)	qM_2 (ms^{-2})	M_c(nmr) (g mol^{-1})
36	0.1	100	8.4	10.3	5.8	91.8	0.1515	12 100
5	0.3	109	11.3	7	4.2	88.4	0.3293	8200
48	0.3	28.6	3.4	9.4	5.1	96.3	0.224	9950
46	0.5	31.8	5.3	11	20.2	94.2	0.1285	13 100
44	0.6	39	4.4	12.2	38.6	95	0.1163	13 800
38	0.1	109	3.5	8.6	2.65	96.4	0.3386	8100
40	0.5	30.5	4.1	7.4	7.3	96.4	0.1946	10 700
42	0.7	25	4.9	7.54	13.8	94.4	0.1508	12 100
50	0.3	14	50.3	1.1	—	49.4	5.5	2010
51	0.3	26.5	60	1.4	—	39.7	6.0	1920
52	0.7	13.5	66.5	1.63	—	32.8	6.0	1920

is known that A_f depends on the deformation range and on the swelling degree. Experiments [4] and recent theoretical approaches assume that there is a continuous transition from affine to free-fluctuating behaviour with increasing strain or increasing swelling (high swelling degrees: good solvents, THF and toluene for PDMS; low swelling degrees: bad solvents, acetone, dry samples). We have already shown and discussed a strong dependence of the $RT\rho_P/G^* = M_c$(apparent) on the thermodynamic quality of the swelling agent [4]. In good agreement with these former results we found an increase of M_c(apparent) with increasing swelling degree for unimodal samples 5 and 36. This could be understood if we assume a transition from the affine to the free-fluctuating phantom network. In the theta solvent methylethyl ketone (MEK) (swelling degree ≈ 3.5 for sample 36) the microstructure factor $A_f = 1/2$. In the case of the network series synthesized in the presence of cyclohexane (44, 46, 48) only the dry network shows an affine behaviour. The M_c(apparent) of the bimodal networks is independent of the swelling degree [28]. According to Schimmel and Heinrich [27] we assume free-fluctuating properties. Only sample 42 shows a behaviour similar to that of unimodal samples. The reason for this could be the small amount (only 9 wt%) of a second polymer.

The conditions during the crosslinking reaction influence the behaviour (swelling degree) of a network. Dušek and Prins defined the memory term η as the ratio of the mean square end-to-end distance of an elastic chain in the dry network (d) to the mean square end-to-end distance of a free chain (0) at the concentration at which the network was formed [29]:

$$\eta = \langle r_d^2 \rangle / \langle r_0^2 \rangle = \phi_{polymer}^{2/3} \qquad (12)$$

Eq. (12) is only valid if $\langle r_0^2 \rangle$ is independent of the polymer concentration (theta condition) [30].

Table 2 shows a review of the measured molecular weights between two crosslinks using the nmr and the compression methods.

5. Nmr characterization of the dry PMDS networks

For elastomers well above T_g molecular motions reduce considerably the broadening effect arising from the anisotropic interaction undergone by nuclear spins. The observed residual linewidths are due to rapid anisotropic segmental motions spatially inhibited by chemical crosslinks, topological chain constraints such as physical and chemical interactions acting as anchors for the rapid short-range processes. The measured decay of the transversal proton magnetization was fitted by Eq. (9). Usually the long exponential tail of the decay due to some free chains (sol content, portion C with the relaxation time $T_{2, sol}$) is removed by substraction of an exponential function before fitting. Thus, in total, four independent parameters remain as fitting parameters: qM_2, T_2, A, ($B = 1 - A$) and τ_{slow}. From the fitted parameter qM_2 the mean average molar mass between two crosslinks M_c can be calculated using Eq. (10). The anisotropy of the motion, and therefore the residual part of the dipolar interaction, increases with increasing network density. The estimated values of the mean molar mass between two crosslinks M_c coincide within $\pm 15\%$ error with the M_c values obtained from compression measurements (with the exception of samples 44, 46 and 48). Simon et al. [5] found, for endlinked model PDMS networks, an acceptable agreement between the M_n values of the precursor chains and the M_c from nmr relaxation measurements. For the PDMS under study, an agreement between the M_n values of the precursor chain resulting from SEC and the nmr-M_c was expected only in first approximation. This is probably caused by the broad molar mass distribution (which is much broader then in Ref. [1]; see Table 1) and the crosslinking reaction. Sol content C (free chains) is negligible in this system owing to the extraction procedure. However, a small portion of dangling ends (portion B) of about 7% is obtained; this may result from the extraction procedure in toluene due to chain scission at the large swelling degree in this solvent.

Based on the model used, the fit with Eq. (9) yields additionally two correlation times: one describes a rapid segmental (liquid-like) but anisotropic motion due to the topological constraints (τ_{fast}, calculated from the fit
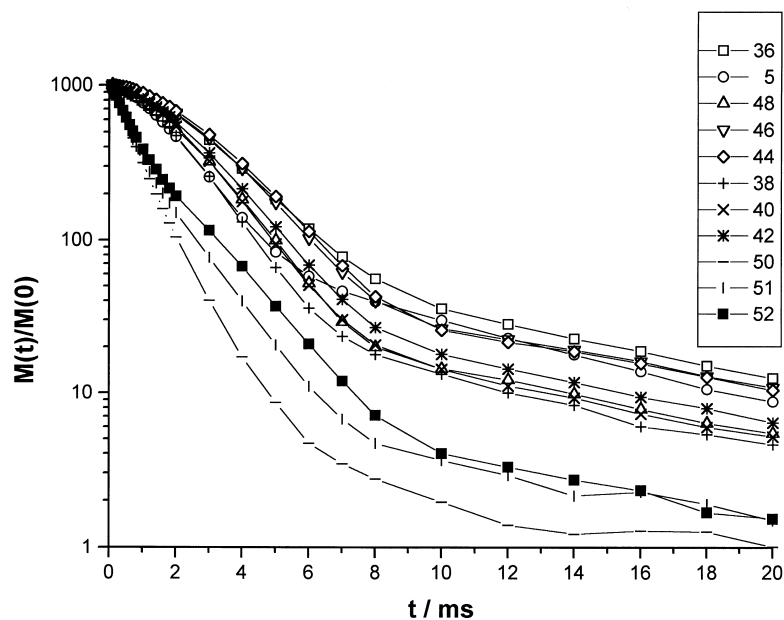
Fig. 1. Decay of proton transversal magnetization versus echo time for all investigated dry networks (for sample no. see Table 2).

parameter T_2 using Eq. (6)); the other one has a more trial character (τ_{slow}, e.g. additional averaging of dipolar interaction due to the larger-scale motions or fluctuations). The differences in τ_{fast} (or T_2) are small because of its local character but with a small tendency to increase (or decrease) towards larger network density. The largest effect on the chain mobility was found in the networks with different 'memory term' (44, 46, 48) expressed in τ_{slow}. In these networks the degree of motional anisotropy is reduced towards lower η-values in comparison with the corresponding sample no. 5 (due to larger fluctuating regions). That means at the same time a decrease in the mutual hindrance

of the chain-movements. Different swelling degrees Q were achieved at the same precursor chain length depending on η. A raised η yields a lower Q in the same solvent.

The results obtained from a fit of Eq. (9) to the experimental magnetization decay are summarized in Table 3. Dramatic differences in the shapes of the curves are only observed for some samples with a bimodal distribution of precursor length (sample nos 50–52) as is shown in Fig. 1. A very fast decay of magnetization is observed at short echo times which is mainly effected by a polymer component with a very short chain length. Therefore, a correct network density was difficult to estimate in these bimodal samples
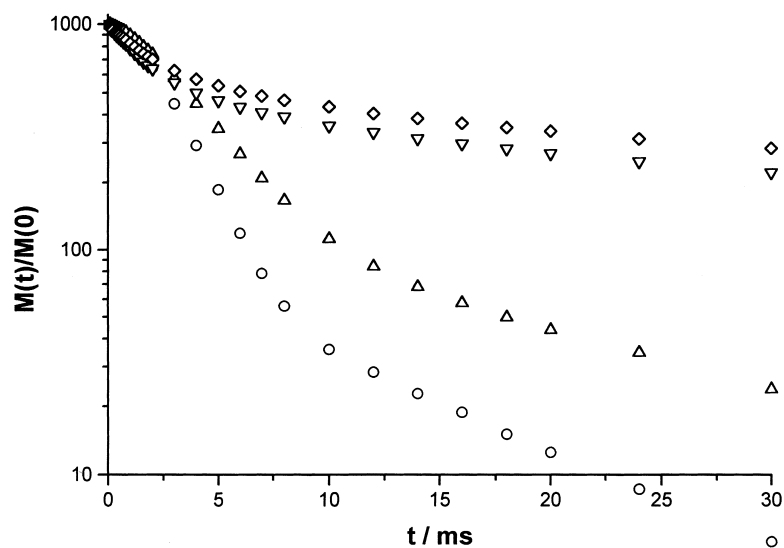

Fig. 2. Decay of proton transversal magnetization versus echo time of sample no. 36 swollen in different solvents (○, dry network; △, swollen in acetone; ▽ swollen in THF; ◇ swollen in toluene).
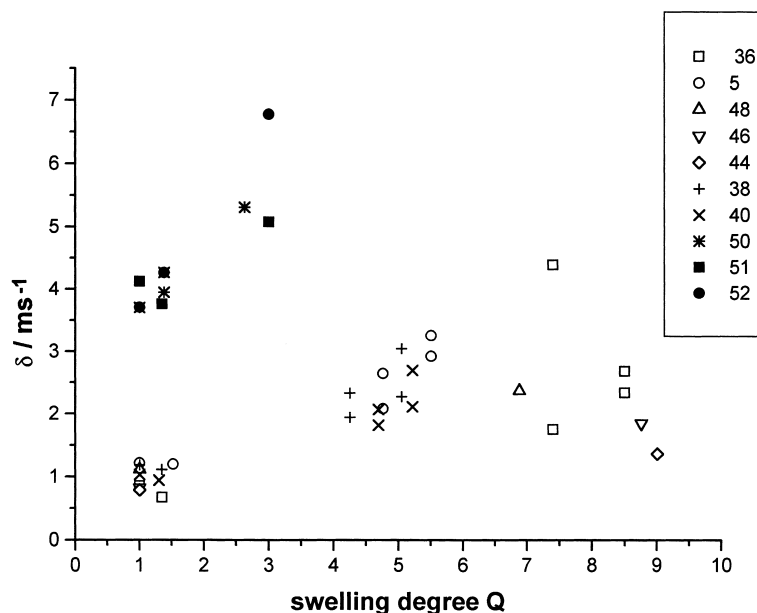
Fig. 3. Parameter δ versus swelling degree Q for different samples (for sample no. see Table 2).

from the nmr relaxation measurements due to the dominant role of anisotropy. For the fitting procedure of these samples the limit $\tau_{slow} \ll t$ of Eq. (9) was assumed. In the bimodal samples the residual interaction is strongly influenced by the component with the shorter precursor chain length. The larger the amount (polymer 4) of longer chains (sample nos 38, 40, 42) the more pre-averaged is the dipolar interaction. In contrast, there is nearly no influence on the residual dipolar interactions of the protons (expressed in $M_2^{Res} = qM_2$) in dependence on the length of the precursor chains of the second component (sample nos 50, 51, 52).

6. Equilibrium swelling of polymer networks: nmr observation

The nmr measurements were performed on samples with different crosslink densities swollen to equilibrium by an excess of deuterated solvent in order to obtain different swelling degrees Q. The decays of the transversal proton magnetization are shown in Fig. 2 and correspond to a medium crosslinked sample swollen in different solvents. Overall, the behaviour is the same for all samples investigated, with some deviations in the above-mentioned short component bimodal networks (sample nos 50, 51, 52). However, there are changes in the shape of the relaxation decay depending on the realized degree of swelling. If acetone is used ($Q \sim 1.4$ for sample 36), the samples are only slightly swollen. Then the shape is still Gaussian as in the dry network, but the 'non-averaged second moment' $M_2^{Res} = qM_2$ as a measure of the residual dipolar interaction is somewhat reduced. On the other hand, when, using toluene or THF in order to obtain a larger degree of swelling
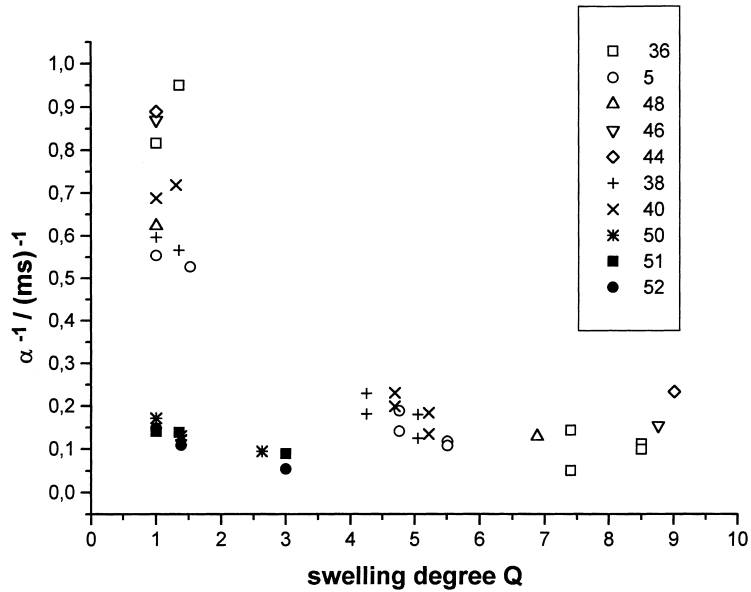
(for sample 36 $Q = 7.4$ or 8.5 respectively) then the relaxation curve changes dramatically. A distinct increase in the 'non-averaged second moment' is observed, as shown in the fast decay at the beginning of the curve (Fig. 2), which is due to the strong isotropic deformation. Large changes in the behaviour are expected in the Q-range of about 3–5, indicating a 'cross-over' due to a possible two-step swelling process. At the first stage, ranging from $Q \simeq 1$ to about $Q \simeq 3$, there is a decrease of residual dipolar interaction (decrease of qM_2). In the second range (larger Q) there is an increase of the residual anisotropy expressed in qM_2.

Simultaneously, with all samples an increasing amount of the tail of relaxation was observed. This decays more slowly for the weakly crosslinked samples. The decay becomes slower with increasing degree of swelling. This behaviour has already been observed in PDMS and SBR using tetrachloroethylene as the swelling agent.

An analysis by Eq. (9) only applies to the less swollen samples. At large Q-values the curves are similar to those of the dry bimodal samples mentioned above. A tentative fit was tried in the limit of $\tau_{slow} \ll t$ of Eq. (9) in order to get some more information. The results show a growing anisotropy and hindrance of motion due to further swelling. The calculated nmr-M_c values for the samples swollen in acetone should be handled with care. This is because Eq. (10) originally did not take into consideration any isotropic deformation but, on account of the swelling ratios being close to unity, the values could be used as first approximation.

To illustrate the effect of residual dipolar interaction on the relaxation function, firstly, the analysis of measured relaxation functions was attempted by a series expansion in terms of second and higher moments imposed by nuclear relaxation theory.

Fig. 4. Parameter α^{-1} versus swelling degree Q for different samples (for sample no. see Table 2).

The relaxation function could be expressed as

$$M(t) = 1 - (M_2/2)t^2 + (M_4/4!)t^4 + ... \quad (13)$$

where now M_2 and M_4 are known to be respectively the second and fourth Van Vlecks moments of the corresponding resonance lines [13,19,31].

The second moment is not affected by molecular motions and is directly related to the residual dipolar interaction Δ_r. For pure dipolar interactions the relationship $M_2 \propto \Delta_r^2$ is valid.

While testing several fitting functions Cohen-Addad and coworkers proposed an empirical function $G_{(\delta\alpha)}(t)$ to

describe the relaxation decay [13,31]:

$$G_{(\delta\alpha)}(t) = \exp\{ - \delta^2/\alpha^2[\log(1 + \alpha t + \sqrt{1 + \alpha^2 t^2}]^2\} \quad (14)$$

which corresponds to the following expansion near the origin ($\alpha t < 1$):

$$G_{(\delta\alpha)}(t) = 1 - (2\delta^2) \frac{t^2}{2} + (12\delta^4 + 8\delta^2\alpha^2) \frac{t^4}{4!} + ... \quad (15)$$

with M_2 and M_4 being evaluated by the expressions

$$M_2 = 2\delta^2, \qquad M_4 = 12\delta^4 + 8\delta^2\alpha^2 \quad (16)$$
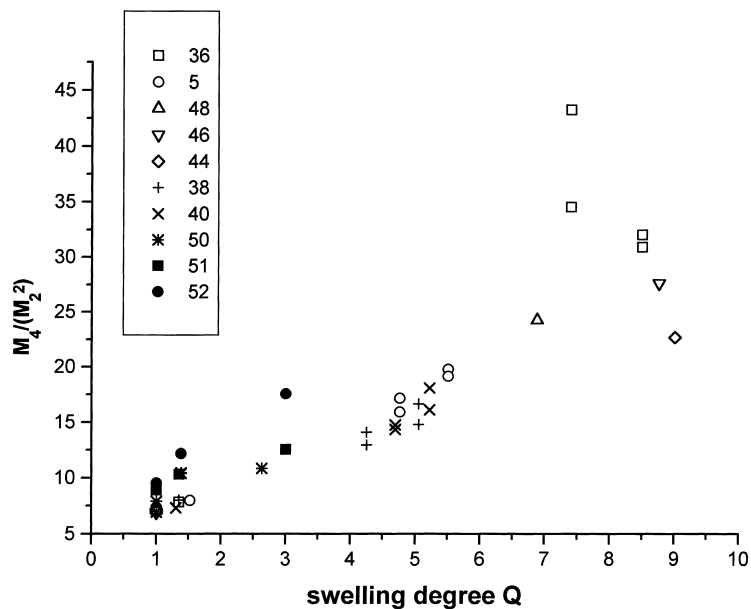
The parameter δ thus reflects the residual dipolar

Fig. 5. Ratio M_4/M_2^2 versus swelling degree Q for different samples (for sample no. see Table 2).

interaction Δ_r and α^{-1} is a fictitious time related to the asymmetry of monomeric diffusive motions. The ratio M_4/M_2^2 indicates the deviation from Gaussian behaviour.

7. Discussion

The values of δ, α^{-1} and M_4/M_2^2 determined as a function of Q are drawn in Figs. 3–5. The parameter δ and the ratio M_4/M_2^2 increase with the swelling degree, but the evolutions of δ and M_4/M_2^2 are in agreement with a two-step process as already observed by Cohen-Addad and coworkers [13,31] in swollen polyethylene networks. The change between both regimes seems to occur at about $Q \sim 3.5$ as discussed earlier [31]. The parameter α^{-1} decreases continuously with increasing swelling degree and seems to reach an asymptotic value at high swelling degrees. This asymptotic value has already been observed for the dry bimodal networks with the very short component (50–52) and is nearly independent from the swelling degree of these samples. On the other hand, the M_4/M_2^2 values of those samples are small and show only a slight increase with Q due to a bad swelling behaviour ($Q_{max} \sim 3.5$). But, the observed values coincide well with those of all other networks in this series.

Only the parameter δ is much larger than those of the other samples and seems to increase linearly with Q, whereas the values are on a level which is reachable for all other samples only at swelling degrees of $Q \gg 8.5$. This effect agrees well with the assumption that the large anisotropy, which is dominant in these polymer networks, is caused by the very short chain length of one of the cross-linked components. Besides the swelling behaviour, this short component has a strong influence on all other properties, as the results from compression measurements indicate.

In the dry state a polymer network is determined by entanglements and chemical crosslinks. When swollen by a low molecular weight solvent, the network structure necessarily unfolds and elementary chains become separated. The presence of a solvent first induces a washing out of unattached chains still remaining after extraction and a reduction of entanglements as far as possible. This could explain the long tail of the relaxation curve as an indication of the amount of free dangling ends. At low swelling degree, the chains remain Gaussian and are not stretched. This stage corresponds to a decrease of residual dipolar interaction or of the 'non-averaged part of the second moment' (qM_2) due to a somewhat better chain mobility, expressed also in some larger T_2-values (shorter τ_{fast}). This relaxation decay may be satisfactorily described by Eq. (9). Further swelling up to $Q \sim 3.5$ leads to a loosening of the structure, unfolded to a maximum degree, compatible with topological hindrances. Thus, the mean distance between two constraints is only determined by real averaged chemical crosslinks or to some extent by 'trapped' entanglements.

Above this Q-value the chains become increasingly stretched. Because of the constant chain length between the crosslinks, this isotropic deformation induces an increase of the anisotropy parameter q (or of the parameter δ). The relaxation tail of more weakly crosslinked samples decays more slowly than those of the more strongly cross-linked one. The motions are increasingly hindered with crosslinking. The bimodal networks with medium chain length of both components (sample nos 38, 40, 42) are found to be between the corresponding unimodal networks (sample nos 5, 36). If one of the components in the bimodal networks is very short (sample nos 50, 51, 52), then the properties are mainly determined by a large degree of anisotropy of motion and less by the swelling behaviour caused by the small mesh size of some parts or a distribution of chain length between two crosslinks. The solvent then affects only parts of longer chains within the network. This agrees well with the observed tendency $M_c(\text{apparent}) = f(Q)$ from compression measurements.

It is to be noted here that the agreement between the M_c values determined by nmr and uniaxial compression on the solution-crosslinked networks was not satisfactory. The compression values were calculated considering the memory term. The nmr measurements were evaluated without any correction of an entanglement contribution to the effective crosslink density. The formation of entanglements, including 'trapped' entanglements (critical molecular weight of entanglements in PDMS [32] is about $16\,600\ \text{g mol}^{-1}$), depends on the polymer concentration [33]. The problem of how to consider the memory-term η in terms of Gotlib's nmr relaxation is still under discussion.

Nevertheless, the 'residual non-averaged second moment' $M_2^{Res} = qM_2$, or the residual dipolar interaction, perceived by nmr is sensitive to the swelling process of polymer networks. The dependence of the minimum of the 'non-averaged second moment' qM_2 on the swelling degree Q, compared with the value in the dry network, could give the amount of topological constraints in end-linked polymer networks.

8. Conclusions

In this paper, we have investigated the swelling process of PDMS networks with different crosslink densities, molecular weight distribution and memory terms. The results of nmr and compression measurements were comparable and support the assumptions about the microstructure factor A_f used in the analysis of the compression measurements.

A satisfactory agreement of mean molar masses between crosslinks M_c in the dry networks determined by nmr and compression measurements was achieved ($\pm 15\%$) with the exception of the solution-crosslinked samples. Both methods are sensitive to the swelling process. The compression results of the unimodal samples 5 and 36 agree well with former results [4], indicating changes in the swelling behaviour at $Q \sim 3$ due to a transition from affine ($A_f = 1$) to

free-fluctuating limit $A_f = (1 - 2/f)$. In the short bimodal networks the mobility of the longer chains is extremely restricted by the shorter ones, so that in the dry state a larger degree of anisotropy of the motion and a strong mutual hindrance of chain movement was already found. Therefore, in this type of bimodal network, no transition between the affine and the free fluctuating limit depending on the swelling degree Q was observed. The occurrence of this transition in the Q-range is strongly influenced by the anisotropy of the polymeric network chain motion and depends on the precursor chain length and the history (memory term).

Acknowledgements

References

[1] Gumbrell SM, Mullins L, Rivlin RS. Trans Faraday Soc 1953;49:1495.

[2] Allen G, Kirkham MJ, Padget J, Price C. Trans Faraday Soc 1970;67:1278.

[3] Zhao Y, Eichinger BE. Macromolecules 1990;22:4507.

[4] Arndt K-F, Galinsky G. Polymer Bulletin 1994;32:103–109.

[5] Simon G, Birnstiel A, Schimmel K-H. Polymer Bulletin 1989;21:235.

[6] Simon G, Götschmann B, Matzen D, Schneider H. Polymer Bulletin 1989;21:475.

[7] Gronski W, Hoffmann U, Simon G, Wutzler A, Straube E. Rubber Chem Techn 1992;65:63.

[8] Heuert U, Knörgen M, Menge H, Scheler G, Schneider H. Polymer Bulletin 1996;37:489.

[9] Simon G, Schneider H. Makromol Chem Macromol Symp 1991;52:233.

[10] Simon G, Gronski W, Baumann K. Macromolecules 1992;25:3624.

[11] Kuhn W, Barth P, Hafner S, Simon G, Schneider H. Macromolecules 1994;27:5773.

[12] Sotta P, Fülber C, Demco DE, Blümich B, Spiess HW. Macromolecules 1996;29:6222.

[13] Cohen-Addad JP. NMR and fractal properties of polymeric liquids and gels. In: Emsley JW, Feeney J, Sutcliff LH, editors. Progress in NMR spectroscopy. Oxford: Pergamon Press, 1993 (and references therein).

[14] Lee S, Pawlowski H, Coran AY. Rubber Chem Technol 1994;67:854.

[15] Matzen D, Straube E. Colloid Polym Sci 1992;270:1.

[16] Malveau C, Tekely P, Canet D. Solid State Nucl Magn Res 1997;7:271.

[17] Callaghan PT, Samulski ET. Macromolecules 1997;30(1):113.

[18] Ball RC, Callaghan PT, Samulski ET. J Chem Phys 1997;106:7352.

[19] Abragam A. The principles of nuclear magnetism. London: Oxford University Press, 1961.

[20] Kuhn W, Grün F. Kolloid Z 1942;101:248.

[21] Slichter CP. Principles of magnetic resonance. Springer, 1992.

[22] Fedotov VD, Schneider H. In NMR basic principles and progress, vol. 21. Springer, 1989.

[23] Fedotov VD, Tshernov VM, Khasanovitsh TN. Vysokomol Soedin A 1978;XX(4):919.

[24] Gotlib YuYa, Lifshitz MI, Shevelev VA, Lishanskij IS, Balanina IV. Vysokomol Soedin A 1976;XXVIII(10):2299.

[25] Schneider H, Menge H, Knörgen M, Heuert U. In preparation.

[26] Queslel JP, Mark JE. Chapter 9. In: Allen G, Bevington JC, editors. Comprehensive polymer science, vol. 2. Oxford: Pergamon Press, 1988:271–309.

[27] Schimmel K-H, Heinrich G. Colloid Polym Sci 1991;269:1003.

[28] Arndt K-F, Pönitzsch S. In preparation.

[29] Dušek K, Prins W. Fortschr Hochpolym Forsch 1969;6:6.

[30] Rennar N, Oppermann W. Colloid Polym Sci 1992;270:527.

[31] Schmit C, Cohen-Addad JP. Macromolecules 1989;22:142.

[32] Plazek J, Riande E, Markovitz H, Raglupathi N. J Polym Sci Polym Phys Ed 1979;17:2189.

[33] Urayama K, Kohjiya S. J Chem Phys 1996;104:3352.